The Influence of Surface Texturing and Boundary slip on the Film Thickness in Parallel Sliding Surfaces

Conference Paper · January 2018

CITATIONS
0

READS
75

3 authors, including:

Dariush Bijani
University of Twente
5 PUBLICATIONS **8** CITATIONS
SEE PROFILE

Loredana Deladi
Robert Bosch GmbH
9 PUBLICATIONS **57** CITATIONS
SEE PROFILE

The Influence of Surface Texturing and Boundary slip on the Film Thickness in Parallel Sliding Surfaces

Dariush Bijani[1)*], M.B. de Rooij[1)] , E.L. Deladi[2)] and D.J. Schipper[1)]
1) University of Twente, Faculty of Engineering Technology, Laboratory for Surface Technology and Tribology, Drienerlolaan 5, 7500 AE Enschede, The Netherlands
2) Bosch Transmission technology, Dr. Hub Van Doorneweg 120, 5026 RA, Tilburg, The Netherlands

*Corresponding author. Email: d.bijani@utwente.nl

Abstract
Considering the influence of wall slip on fluid flow is important for many engineering topics involving liquid-solid interfacial phenomena, such as flow through porous media, liquid coatings and lubrication. Boundary slip can act as a method to reduce friction in lubricated contacts. Furthermore, surface texturing can also play a positive role to enhance the film thickness. Therefore, combination of these two methods can be beneficial in order to improve the tribological performance of lubricated contacts. Although, in recent years the study of frictional behaviour of surface with boundary slip is getting more attention, the combination of these two methods of surfaces properties modification is interesting to investigate. For the no-slip boundary condition, the first layer of fluid molecules has the same velocity as the contacting solid surface and this condition has been widely applied in the field of fluid mechanics. In lubricated contacts with boundary slip, the first layer of the lubricant molecules move with a different velocity from that of the solid surface. In this article, the frictional behaviour of boundary slip in parallel sliding lubricated contacts for textured surfaces is investigated. This study shows that boundary slip has a significant influence on the film thickness in case of textured surfaces. Furthermore, it is possible to increase the film thickness, and enhance the frictional behaviour by modifying the boundary slip parameters.

Keywords
Hydrodynamic lubrication; surface texturing; boundary slip; film thickness; texturing patterns; numerical modeling

Nomenclature

Parameters	Description	Unit
h	film thickness	m
h_0	Contact separation	m
u_0	Sum velocity	m/s
P	Dimensionless pressure	$-$
p	Pressure	Pa
p_a	Ambient pressure	Pa
p_c	Cavitation pressure	Pa
η	Dynamic viscosity	$Pa.s$
ρ	Lubricant density in full film region	$Kg/m3$
F	Elrod cavitation algorithm switch function	$-$
φ	Cavitation dimensionless variable	$-$
b	Slip length	m
u_s	Slip velocity in x-direction	m/s
v_s	Slip velocity in y-direction	m/s
τ_{xz}	Shear stress	kPa
τ_{cx}	Shear stress x-component when slip takes place at solid surface	kPa
τ_{co}	Critical shear stress	kPa
T_d	Texture depth	m
r_p	Cavity characteristic width	m
S	Cavity size = $2r_p$	m
P_x	Texture pitch	$-$
L	Contact length	m

L_s	Slip area length	m
L_{gx}	Texture cell length in x-direction	m
L_{gy}	Texture cell length in y-direction	m
L_x	Textured area in x-direction	m
L_y	Textured area in y-direction	m
X	Dimensionless Cartesian coordination = $\mathrm{x}/\mathrm{r_p}$	$-$
Y	Dimensionless Cartesian coordination = $\mathrm{y}/\mathrm{r_p}$	$-$
H	Dimensionless local depth of textured surface	$-$
μ	Coefficient of friction	$-$
μ_{ref}	Coefficient of friction for reference condition	$-$
μ^*	Normalized coefficient of friction for slip length study = μ/μ_{ref}	$-$

1. Introduction

In the case of no-slip boundary condition, the immediate layer of the fluid next to the solid surface moves with the same velocity of contacting solid surface. This boundary condition is employed universally for much sophisticated calculation in fluid mechanics [1]. However, there have been doubts about its validity [2-6]. In studies with measurement of velocity gradients in fluids [7, 8] and measurements studying non-wetting on viscous shear forces [9, 10] confirmed that, slip happened when the surface is smooth and the fluid is weakly bonded to the solid [7, 8, 11-13]. Furthermore, Spikes [14, 15] showed that due to wall slip, it is possible to achieve interesting opportunities for hydrodynamic bearing design, in particular in the lubrication of microelectromechanical systems (MEMs).

In the study of Tauviqirrahman et al. [16], the effect of boundary slip on friction reduction is investigated. In that study a combined optimized complex slip surface and an optimized slope incline ratio is obtained. It was shown that surface optimization of a parallel sliding gap with a slip surface can double the hydrodynamic load carrying capacity and reduce the friction force by an half of what the classical Reynolds theory predicts for an optimal slope inclination of a traditional sider contact. For a two-dimensional (finite length) journal bearing Ma et al. [17] showed that the optimization of shape and size of the surface may enhance the frictional behaviour.

It has been found that some non-Newtonian liquids such as polymer melts show boundary slip effects at solid surfaces. This boundary slip is due to reduction in viscosity of the fluid layer close to the surface as a result of shear thinning or compositional variation [18-21]. In these cases, slip has been modeled by the Navier slip length model. The results in these studies show an agreement to the predictions and measurements [1].

For Newtonian liquids, the results were compared with this Navier model. Some studies obtained results fitting closely to the constant slip length model [7, 8, 13] but others not f [12, 22-24].

To solve this issue, a wall slip model is developed by Spikes [15] in which a critical shear stress criterion is broadened to incorporate both a critical shear stress and a constant slip length criterion. This combined model is compared with experimental and showed rather good agreement.

In work of Tauviqirrahman et al. [25, 26] they showed that when the surface has partially boundary slip, it is possible to improve the performance of fluid bearings by increasing the lubricant film thickness due to the higher load carrying capacity generation. In these studies, the lubricated sliding contact is operating under steady state conditions.

The focus of this study is to develop a model to calculate the film thickness and predict the frictional behaviour of contacts in case of parallel textured sliding contacts, including boundary slip. In this model, the decisive effect of cavitation due to texturing is also applied.

2. Mathematical solution

Experimental studies with wall slip make use of surfaces with different physical or chemical treatments together with different types of lubricants in order to achieve different solid/liquid interfacial properties. Another common means to change the property of the solid/liquid interface is by addition of surfactants to the liquid lubricant. The velocity of the fluid flow at the wall surface can be effectively adjusted by putting different concentrations of surfactants [24].

In order to simulate the boundary slip phenomenon the main challenge is choosing the most realistic slip model and employing the most accurate boundary conditions for a hydrophobic surface.

There are two main wall slip models which have been adopted to describe the boundary slip, i.e. the slip length model (SLM) and the critical shear stress model (CSSM)[16].

- **Slip length model (SLM):**

A boundary condition for partial slip was proposed by Navier in 1823. This boundary condition is the most frequently used model to characterize boundary slip. Navier introduced a linear boundary condition, which state that the liquid velocity term $u_{z=0,h}$ at the wall surfaces is proportional to the shear stress at the surface. The slip length, b, which is defined as the distance beyond the liquid/solid interface as shown in Fig. 1.b.

$$u_{z=0,h} = u_s = b\frac{\tau_x}{\eta} = b\frac{du}{dz}|_{z=0,h} \quad (1)$$

Where:
b: Slip length,
u_s: Slip velocity of the fluid along the surface x-axis,
u: Velocity component in x-direction,
η: Bulk viscosity,
τ_x: Shear stress in x-direction.

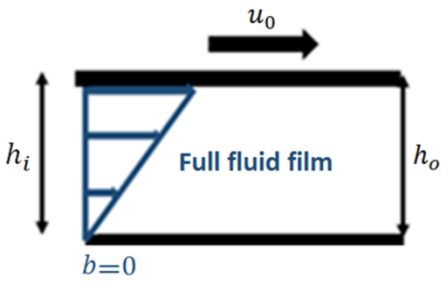

(a)

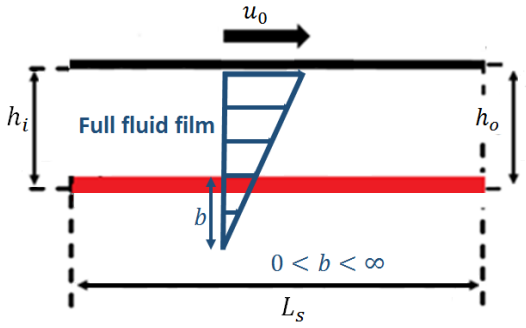

(b)

Figure 1: Schematic of wall slip model. (a) No-slip, (b) Boundary slip condition.

- **Critical shear stress model (CSSM):**

Spikes and Granick [1] introduced a new mathematical slip model for Newtonian fluids. Their model $\tau_c = \tau_{co} + \frac{\eta}{b}u_s$ incorporates both the critical shear stress and constant slip length criteria in which τ_{co} is the critical shear stress at the onset of slip. The critical shear stress model adopted in the present study assumes that wall slip occurs only after the surface shear stress reaches the critical shear stress. The focus of this section is to show the importance of the critical shear stress choice for contacts with a textured surface combined with a slip boundary.

2.2 Governing equations

Based on the force equilibrium analysis of a fluid element one obtains (1-D):

$$\frac{\partial p}{\partial x} = \frac{\partial \tau}{\partial z} \quad (2)$$

For Newtonian flow:

$$\tau = \eta\frac{\partial u}{\partial z} \quad (3)$$

Substituting Eq. 2 in Eq. 3 and by applying the flow continuity the result is:

$$\rightarrow \frac{\partial q_x}{\partial x} + \frac{\partial q_y}{\partial y} = 0 \rightarrow \frac{\partial}{\partial x}\left(\frac{-h^3}{12\eta}\frac{\partial p}{\partial x}\right) + \frac{\partial}{\partial x}\left(\frac{h}{2}(U+u_s)\right) + \frac{\partial}{\partial y}\left(\frac{-h^3}{12\eta}\frac{\partial p}{\partial y}h^3\right) + \frac{\partial}{\partial y}\left(\frac{v_s h}{2}\right) = 0$$
$$\frac{\partial}{\partial x}\left(h^3\frac{\partial p}{\partial x}\right) + \frac{\partial}{\partial y}\left(h^3\frac{\partial p}{\partial y}\right) = 6\eta\left(u_0\frac{\partial h}{\partial x} + \frac{\partial(hu_s)}{\partial x} + \frac{\partial(v_s h)}{\partial y}\right) \quad (4)$$

By defining the following dimensionless parameters:

$$X = \frac{x}{L}, Y = \frac{y}{B}, H = \frac{h}{h_0}, U_s = \frac{u_s}{u_0}, V_s = \frac{v_s}{u_0}, P = \frac{p-p_c}{p_a}, W = \frac{6\eta u_0 L^2}{p_a h_0^2}$$

Eq. 4 becomes:

$$\frac{\partial}{\partial X}\left(H^3\frac{\partial P}{\partial X}\right) + \frac{L^2}{B^2}\frac{\partial}{\partial Y}\left(H^3\frac{\partial P}{\partial Y}\right) = W\left(\frac{1}{L}\frac{\partial H}{\partial X} + \frac{1}{L}\frac{\partial(HU_s)}{\partial X} + \frac{1}{B}\frac{\partial(HV_s)}{\partial Y}\right) \quad (5)$$

2.3 Boundary conditions

2.3.1 Slip Length Model (SLM)

By applying the boundary slip, on the stationary surface it is possible to increase the beneficial effects of this phenomenon [16, 25-27] to achieve a higher load carrying capacity for the parallel sliding surface situation (see Fig. 2). In addition, the slip area is starting from the point that the flow is starting to enter into the first cavity, the reason to use this geometry is to apply the effect of partial slip. Furthermore, the optimum slip area dimensions from work of Tauviqirrahman et al. [28] is applied to achieve a higher film thickness. Tauviqirrahman et al. [25] showed that in their study, which in order to achieve a thicker lubricant film the optimized partial slip is beneficial. Therefore, for the boundary conditions for slip area we have:

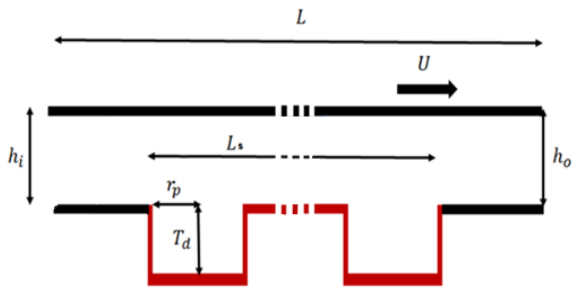

Figure 2: The schematic parallel sliding contacts, the red lines are showing the surfaces with boundary slip effect.

$$\begin{cases} z = h \rightarrow u = u_s, v = v_s \\ z = 0 \rightarrow u = u_0, v = 0 \\ h_i = h_o = h \end{cases} \quad (6)$$

2.3.2 Critical Shear Stress Model (CSSM)

From the two-component slip model reads:

$$\tau_c = \tau_{co} + \frac{\eta}{b} u_s \quad (7)$$

From the boundary conditions in the case that the slip occurs at the lower stationary surface, the upper and lower surfaces boundary condition reads:

$$\begin{cases} z = 0;\ no - slip\ boundary\ condition \\ \quad \rightarrow u = u_0,\ v = 0 \\ \\ z = h;\ Slip\ boundary\ condition \\ \quad \rightarrow u = u_s,\ v = v_s \end{cases} \quad (8)$$

Which in Eq. 7, $h_i = h_o = h$ and $\tau = \tau_{cx}$ when $z = h$.

$$\frac{\partial p}{\partial x} = \frac{\partial \tau_{xz}}{\partial z} \text{ and} \quad (9)$$
$$\tau_{xz} = \eta \frac{\partial u}{\partial z} = \frac{\partial p}{\partial x}(z - h) + \tau_{cx}$$
$$\rightarrow u = u_1 + \frac{1}{\eta}\frac{\partial p}{\partial x}\left(\frac{z^2}{2} - hz\right) + \frac{\tau_{cx}}{\eta} z$$

Calculating u_s from the two component model of Spikes and Granick [29] (Eq. 4) and by applying the boundary conditions (Eq. 9):

$$u_s = \frac{\left(u_0 - \frac{h^2}{2\eta}\frac{\partial p}{\partial x} - sgn(u_s)\frac{h}{\eta}\tau_{co}\right)}{1 + \frac{h}{b}} \quad (10)$$

2.4 Friction calculation

In these simulations to calculate the coefficient of friction, we have:

$$\mu = \frac{F_f}{W} \quad (10)$$

Where, the friction force (F_f) generated in a lubricated system is due to shearing the fluid. By integrating interface shear stress over the interface surface area, the friction force (F_f), is obtained:

$$F_f = \int_0^w \int_0^l \tau dx dy \quad (11)$$

Where, (l) is the length and (w) is the width of surface. In addition, load support (W), is obtained by integration of the pressure:

$$W = \int_0^w \int_0^l p dx dy \quad (12)$$

Therefore, in order to calculate the coefficient of friction, we have:

$$\mu = \frac{\eta u_0}{ph} \quad (13)$$

In this study in order to have a better understanding of boundary slip effect on textured surfaces on frictional behaviour of contacts the normalized coefficient of friction can be employed. The normalization of coefficient of friction is possible by dividing the calculated coefficient of friction over a reference coefficient of friction. The reference coefficient of friction can be deferent in different type of calculations.

$$\mu^* = \frac{\mu}{\mu_{ref}} \quad (14)$$

2.5 Solution

There are two groups of approaches in solving (Eq. 5), i.e., the direct solvers and the iterative solvers. Further, it is more common to utilize the de-coupled iteration technique rather than the fully coupled iteration technique. In order to solve this modified Reynolds equation in large-scale lubrication problems, iterative solvers are more applicable because they avoid the storage requirement that a direct solver generally demands. Iterative solvers include nodal iteration, the tri-diagonal matrix algorithm (TMDA) (Patankar [30]). TDMA, also known as the Thomas algorithm, is a simplified form of the Gaussian elimination to solve the tri-diagonal systems of equations. It breaks the problem into a series of tri-diagonal sub-problems where any entries outside the tri-diagonal portion are treated as source terms using the previous values. When one solves a two-dimensional problem, the TDMA solution column by column or row by row becomes iterative, and sweeping is done line-by-line and column-by-column or row-by-row. Supposing the domain is discretized by $n_{nodes} = n_{col} \times n_{row}$ nodes.

In this case, the computed domain should be divided into a number of control volumes and the modified Reynolds equation will be solved using a TDMA. In the two-dimensional case, it is possible to solve the equations iteratively for the pressure at each grid point using the alternating-direction-implicit (ADI) method with the tri-diagonal-matrix-algorithm (TDMA). The numerical solution is schematically is presented in the fellow chart in appendix A.

3. Results and discussion

In work of Tauviqirrahman et al. [16, 25-27] on the effect of boundary slip in contribution with textured surfaces, the influence of boundary slip over the load carrying capacity and friction force parameters in textured surfaces has been studied. Although they solved the modified Reynold equation, the effect of cavitation was neglected. Therefore, in this study by applying the boundary slip equations in film thickness model a three-dimensional model for boundary slip developed which it contains the effect of cavitation.
In this section, several numerical simulations have been performed to obtain a better understanding on influence of boundary slip parameters over the film thickness in textured surface. In these calculations, the effect of slip length and critical shear stress (τ_{co}) on hydrodynamic film thickness is investigated. In these calculations, the slip area length is equal to 75% of contact length, this decision is made based on the study of Tauviqirrahman et al. [28] on optimization of boundary slip area.

Table 1: range of operating parameters.

Parameter	Value	Unit
Texture depth (T_d)	10	μm
Texture size (S)	150	μm
Texture Pitch (P_x)	0.5	$-$
Viscosity	8	$mPa.s$
Load	20	N
Slip length (b) range	$0-40$	μm
Critical shear stress (τ_{co}) range	$1-2000$	kPa
Slip area length ($\frac{L_s}{L}$)	0.75	$-$
Contact area	1×10^{-6}	m^2

Based on parameters on table 1 several calculations are done in order to find the influence of slip length and critical shear stress on film thickness for textured surfaces. The texturing pattern is shown in Fig. 3.

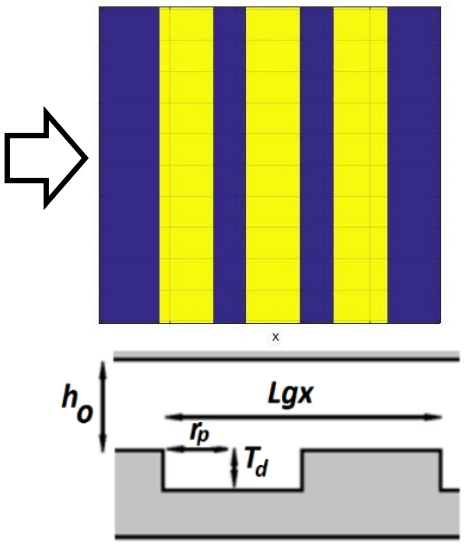

Figure 3: Texture pattern (open groove pattern).

In this study, a rectangular geometry for the texture cell shape is used.
Cavity size: $S = 2 \times r_p$
Pitch in x direction: $P_x = \frac{S}{L_{gx}}$

3.1 Effect of Slip length (b)

Based on the mathematical model and the method of solution for this model, one of the two main parameters that they have control over the wall slip behaviour is slip length. In order to study the influence of this parameter texturing parameters (T_d, S and P_x) and other slip parameter (Critical shear stress, τ_{cs}) are set as constant and the slip length (b) is varying from 0 to $40\mu m$.
As can be seen in Fig. 4, for the textured surface in parallel sliding contact (the wedge effect is absent), the increase of the slip length leads to a sensible improvement in the film thickness. However, in Fig. 4 after slip length is passing $20\mu m$, the growth in this parameter causes a smaller improvement in film thickness in comparison with the values of slip length smaller than $20\mu m$.
The existence of a higher slip length can cause a higher slip velocity on slippery wall, which results on a dramatic velocity difference between the fluid velocity on area with boundary slip and non-slippery areas. This difference in velocity will cause a pressure gradient, which can produce a higher film thickness.

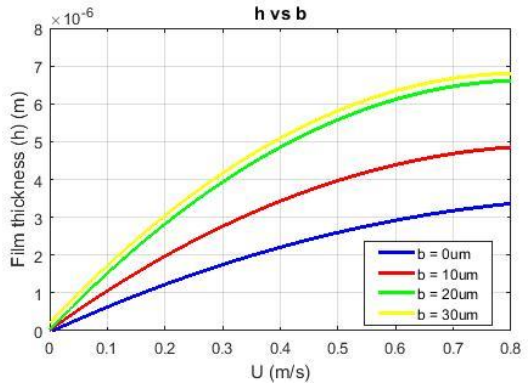

Figure 4: Influence of slip length on film thickness.

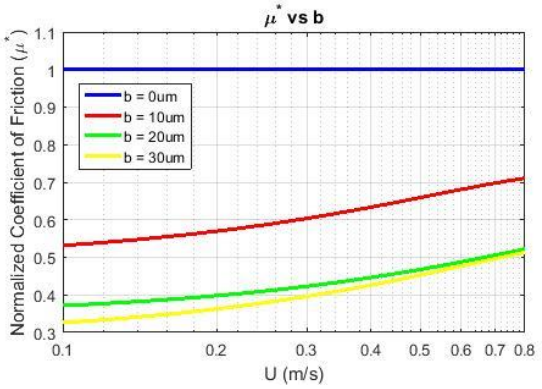

Figure 5: Influence of slip length on friction.

In Fig. 5, the effect of the variation of slip length on frictional behavior of textured surfaces is presented. The coefficient of friction is calculated against the velocities based on four different values of slip length, then by dividing the calculated values over the coefficient of friction in no-slip condition ($\mu_{ref} = \mu_{b=0}$) the normalized coefficient of friction (μ^*) is calculated. This normalization is used to indicate the frictional behaviour of contacts based on different slip lengths.

With respect to normalized coefficient of friction (μ^*), the increase in the slip length leads to a decrease in this parameter (μ^*). It can also be observed, if slip length decreases to zero, then μ^* leads to its no-slip value. It is shown that the rate of friction drop is higher from $b = 0\mu m$ to $b = 20\mu m$ than from $b = 20\mu m$ to $b = 30\mu m$.

3.2 Effect of critical shear stress (τ_{co})

The focus of this section is to show the importance of the critical shear stress to control the frictional behaviour of contacts in case of parallel sliding contact. Therefore, in these calculations the critical shear stress of a partially slip/textured surface is changed between $[1kPa \sim 2Mpa]$ to observe the influence of this parameter over the film thickness and friction. As an observation from Fig. 6, it is possible to obtain that the critical shear stress has a significant effect on the predicted film thickness. It is also possible to observe that by employing a surface with a low critical shear stress ($\tau_{co} = 1\ kPa$ in this case) the highest film thickness is achievable. For a low critical shear stress, more lubricant can enter into the contact, which it results in increasing the hydrodynamic pressure.

The artificial slip surface can be obtained with a super-hydrophobic surface. Therefore, for a higher film formation, it is very beneficial to engineer the critical shear stress to the lowest possible values (i.e. zero critical shear stress equal to perfect slip).

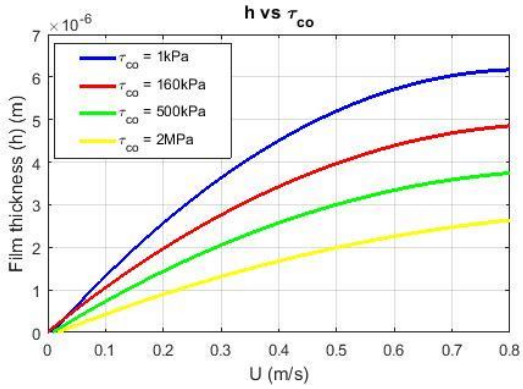

Figure 6: Influence of critical shear stress on film thickness.

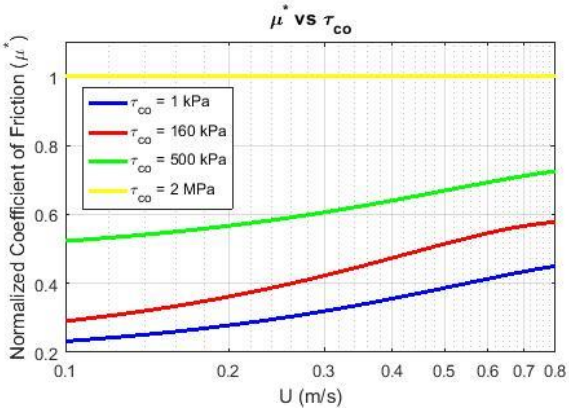

Figure 7: Influence of critical shear stress on friction.

By increasing the critical shear stress value, over the slippery surface the shear stress between the lubricant and wall is increasing this growth means more resistance against the fluid flow in contact area, which results on a lower slip velocity and lower load carrying capacity. Therefore, by increasing the critical shear stress the film thickness is reducing.

In case of friction against the critical shear stress (τ_{co}), in Fig. 7 the normalized coefficient of friction parameter μ^* is used. In order to normalize the coefficient of friction in this part, the highest coefficient of friction calculated which it is when $\tau_{co} = 2\ MPa$ is taken as the reference coefficient friction (μ_{ref}) due to this fact which this friction value is more close to the value when there is no boundary slip effect over the surface. From Fig. 7 it is possible to observe that by increasing critical shear stress (τ_{co}) value, the coefficient of friction in textured surfaces are increasing e.g. the lowest normalized coefficient of friction is achievable when τ_{co} is close to zero. Therefore, reducing the critical shear stress value, to a very low

level, that is, close to zero, the boundary slip leads to a significant improvement in reduction of friction.

4. Discussion

The results from numerical calculations in this article showed that, the existence of boundary slip could increase the film thickness and reduce the coefficient of friction. On the other words, with respect to the film thickness, the textured surface with boundary slip is superior to the surfaces with just textured surface.

The existence of boundary slip and slip velocity over the surfaces results in a higher average inlet velocity of lubricant into the contact area. This increase in average velocity causes the growth in fluid flow in the contact region and higher amount of lubricant material in that region will act as an element to have a larger separation between two surfaces; it is possible to translate this higher separation as higher film thickness. Therefore, by increasing the slip velocity it is possible to thicken the lubricant film in contact region.

Rationally, based on terms in Eq. 8, it is possible to observe that the growth of the slip length (b) leads to the increase in slip velocity and film thickness.

Slip length value can control the fluid flow and film thickness in contact region. It is worth to consider that in this study, the full film lubrication (HL) is investigated and in HL regime, the higher values for slip length results in lower coefficient of friction because of a thicker film (see Eq. 13). Therefore, if the reduction of friction in full film lubrication situation is the goal, in presence of surface texturing employing boundary slip is beneficial. On the other hand, by employing the boundary slip it is possible to reach to higher film thickness and as a consequence a higher separation between solid surfaces in contact in lower velocities. Moreover, from Eq. 8, it is also possible to track the effect of critical shear stress in slip velocity, which by decreasing this parameter it is possible to achieve a higher slip velocity and higher film thickness. It is worth to mention that by increasing the velocity the coefficient of friction is also increasing despite the growth of film thickness, because apparently the ratio between the velocity growth is higher than the film thickness growth.

5. Conclusions

The aim of the investigation was to develop a numerical code in order to have a better understanding of film thickness for textured surfaces in boundary slip conditions. The model is based on a numerical algorithm based on Reynolds equation with the Elrod cavitation algorithm formulation. The equations were made discrete using the finite difference method, and solved using the TDMA iterative method. In addition, in order to study the frictional behaviour of parallel sliding contact when the texturing and boundary slip is applied, the normalized coefficient of friction is introduced.

From the study on influence of slip length on film thickness and friction, it is possible to observe that a thicker lubricant film is achievable when the slip length has larger values, due to the higher slip velocity. The positive effect of increasing slip length on film formation is less significant when the value of this parameter is higher than 20μm. With respect to normalized coefficient of friction (μ^*), the increase in the slip length leads to a decrease in this parameter (μ^*). Influence of critical shear stress on film thickness and friction is also studied, based on the calculations it is observed that when the boundary slip effect is present, the highest film thickness is achievable at the lowest values of the critical shear strength. Therefore, by increasing the critical shear stress (τ_{co}) value, the coefficient of friction in textured surfaces are increasing e.g. the lowest normalized coefficient of friction is achievable when τ_{co} is close to zero.

Therefore, from this study it is possible to achieve that the existence of boundary slip can improve the film thickness in case of textured surfaces. In case of boundary slip/textured surface in addition to the geometrical parameters of surface texturing critical shear stress and slip length are two physical parameters, which they have control over the slip and consequently over the film thickness and friction force. Although, by activating the boundary slip in contacts it is possible to reduce the friction and enhance the film thickness, it shall be considered that the slip parameters should be in the optimum range. Based on this study the optimum value for slip length (b) is around $20\ \mu m$. In case of optimum critical shear stress (τ_{co}) from Fig. 7, it is possible to observe that, although the lowest coefficient of friction is achievable when $\tau_{co} = 0kPa$, the rate of friction reduction between $\tau_{co} = 1kPa$ and $\tau_{co} = 160kPa$ is smaller than the rate friction reduction between $\tau_{co} = 160kPa$ and $\tau_{co} = 250kPa$, therefore a critical shear stress around $160kPa$ can be beneficial to decrease the friction in contacts.

6. References

1. Spikes, H. and S. Granick, *Equation for Slip of Simple Liquids at Smooth Solid Surfaces.* Langmuir, 2003. **19**(12): p. 5065-5071.
2. Goldstein, S., *Modern developments in fluid mechanics.* Vol. II, 1938: p. 601-607.
3. Vinogradova, O.I., *Slippage of water over hydrophobic surfaces.* International Journal of Mineral Processing, 1999. **56**(1-4): p. 31-60.
4. Debye, P. and R.L. Cleland, *Flow of liquid hydrocarbons in porous vycor.* Journal of Applied Physics, 1959. **30**(6): p. 843-849.
5. Ruckenstein, E. and P. Rajora, *On the no-slip boundary condition of hydrodynamics.* Journal of Colloid And Interface Science, 1983. **96**(2): p. 488-491.
6. Churaev, N.V., V.D. Sobolev, and A.N. Somov, *Slippage of liquids over lyophobic solid surfaces.* Journal of Colloid And Interface Science, 1984. **97**(2): p. 574-581.
7. Pit, R., H. Hervet, and L. Leger, *Direct experimental evidence of slip in hexadecane: solid interfaces.* Physical review letters, 2000. **85**(5): p. 980.
8. Pit, R., H. Hervet, and L. Léger, *Friction and slip of a simple liquid at a solid surface.* Tribology Letters, 1999. **7**(2-3): p. 147-152.
9. Zhu, Y. and S. Granick, *Limits of the hydrodynamic no-slip boundary condition.* Phys Rev Lett, 2002. **88**(10): p. 106102.
10. Zhu, Y. and S. Granick, *Rate-Dependent Slip of Newtonian Liquid at Smooth Surfaces.* Physical Review Letters, 2001. **87**(9): p. 096105.
11. Boehnke, U.C., et al., *Partial air wetting on solvophobic surfaces in polar liquids.* Journal of Colloid and Interface Science, 1999. **211**(2): p. 243-251.
12. Zhu, Y. and S. Granick, *Rate-dependent slip of Newtonian liquid at smooth surfaces.* Physical Review Letters, 2001. **87**(9): p. 961051-961054.
13. Baudry, J., et al., Experimental Evidence for a Large Slip Effect at a Nonwetting Fluid−Solid Interface. Langmuir, 2001. **17**(17): p. 5232-5236.
14. Spikes, H.A., *The half-wetted bearing. Part 1: extended Reynolds equation.* Proceedings of the Institution of Mechanical Engineers, Part J: Journal of Engineering Tribology, 2003. **217**(1): p. 1-14.
15. Spikes, H.A., *The half-wetted bearing. Part 2: potential application in low load contacts.* Proceedings of the Institution of Mechanical Engineers, Part J: Journal of Engineering Tribology, 2003. **217**(1): p. 15-26.
16. Tauviqirrahman, M., et al., Optimization of the complex slip surface and its effect on the hydrodynamic performance of two-dimensional lubricated contacts. Computers & Fluids, 2013. **79**(0): p. 27-43.
17. Ma, G.J., C.W. Wu, and P. Zhou, *Wall slip and hydrodynamics of two-dimensional journal bearing.* Tribology International, 2007. **40**(7): p. 1056-1066.
18. Schowalter, W.R., *The behavior of complex fluids at solid boundaries.* Journal of Non-Newtonian Fluid Mechanics, 1988. **29**(C): p. 25-36.
19. Léger, L., E. Raphaël, and H. Hervet, *Surface-anchored polymer chains: Their role in adhesion and friction.* Adv. Polym. Sci., 1999. **138**: p. 185-225.
20. Denn, M.M., Extrusion instabilities and wall slip, in Annual Review of Fluid Mechanics. 2001. p. 265-287.
21. Wang, S.Q., Molecular transitions and dynamics at melt/wall interfaces: Origins of flow instabilities and wall slip. Adv. Polym. Sci., 1999. **138**.
22. Craig, V.S.J., C. Neto, and D.R.M. Williams, *Shear-dependent boundary slip in an aqueous Newtonian liquid.* Physical Review Letters, 2001. **87**(5): p. 054504/1-054504/4.
23. Bonaccurso, E., M. Kappl, and H.J. Butt, Hydrodynamic force measurements: Boundary slip of water on hydrophilic surfaces and electrokinetic effects. Physical Review Letters, 2002. **88**(7): p. 761031-761034.
24. Zhu, Y. and S. Granick, No-slip boundary condition switches to partial slip when fluid contains surfactant. Langmuir, 2002. **18**(26): p. 10058-10063.
25. Tauviqirrahman, M., *Lubricated MEMS: effect of boundary slippage and texturing, PhD Thesis*. 2013, Unversity of Twente: Enschede. p. 162.
26. Tauviqirrahman, M., et al., *Combined effect of texturing and boundary slippage in lubricated sliding contacts.* Tribology International, 2013. **66**(0): p. 274-281.
27. Tauviqirrahman, M., et al., *Computational analysis of the lubricated-sliding contact with artificial slip boundary.* International Journal of Applied Mathematics and Statistics, 2013. **35**(5): p. 67-80.
28. Tauviqirrahman, M., et al., A study of surface texturing and boundary slip on improving the load support of lubricated parallel sliding contacts. Acta mechanica, 2013. **224**(2): p. 365-381.
29. Choo, J.H., et al., Friction reduction in low-load hydrodynamic lubrication with a hydrophobic surface. Tribology International, 2007. **40**(2): p. 154-159.
30. Patankar, S.V., *Numerical heat transfer and fluid flow / Suhas V. Patankar*. Series in computational methods in mechanics and thermal sciences. 1980, Washington : New York: Hemisphere Pub. Corp. ; McGraw-Hill.

Appendix A:

The diagram for the methodical solution algorithm used in this study is:

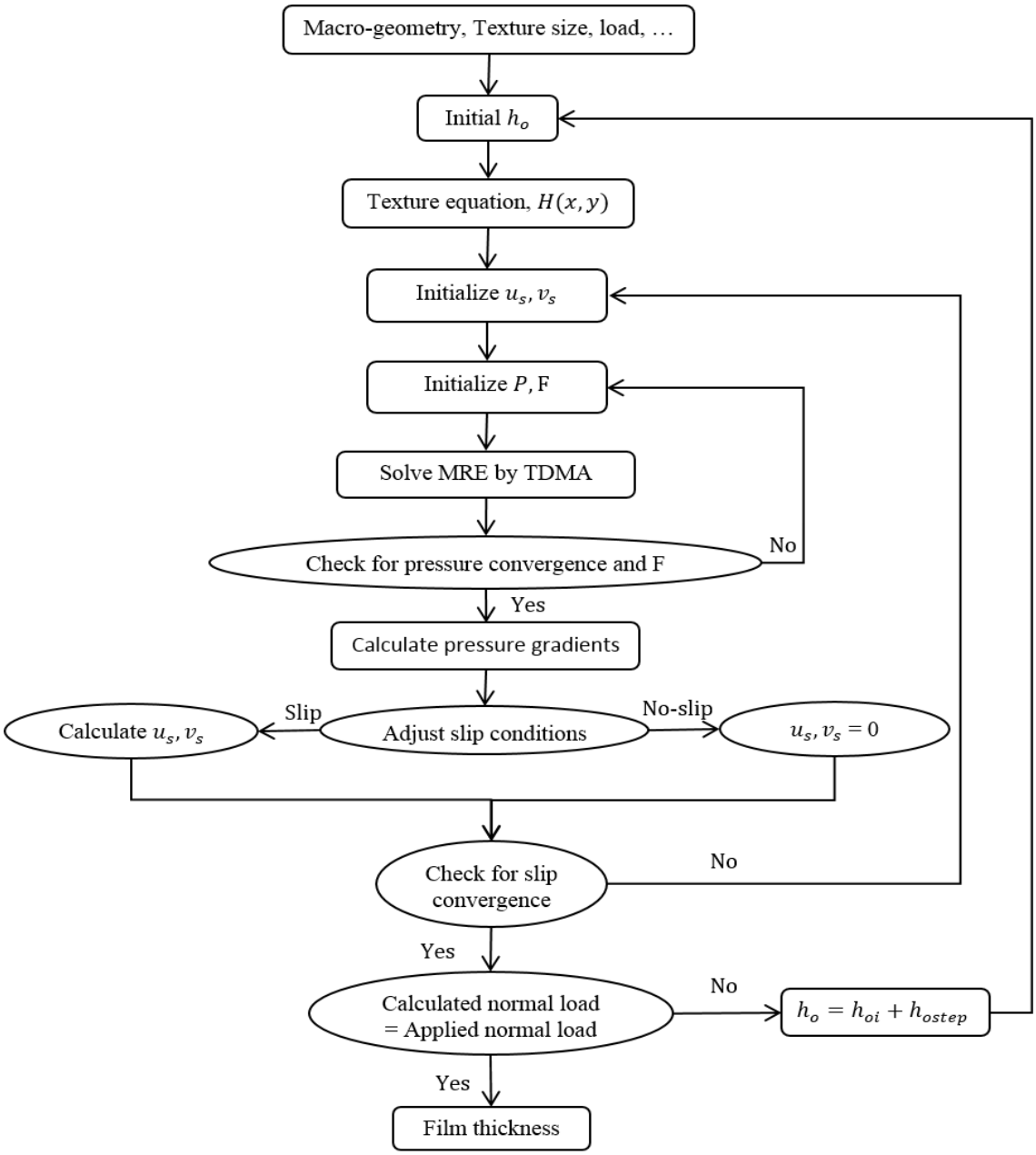

Figure A.1: Solution scheme for numerical calculations.